Editors' Suggestion

Asymmetric Particle Transport and Light-Cone Dynamics Induced by Anyonic Statistics

Fangli Liu,[1] James R. Garrison,[1,2] Dong-Ling Deng,[3,4,1] Zhe-Xuan Gong,[5,1,2] and Alexey V. Gorshkov[1,2]
[1]Joint Quantum Institute, NIST/University of Maryland, College Park, Maryland 20742, USA
[2]Joint Center for Quantum Information and Computer Science, NIST/University of Maryland, College Park, Maryland 20742, USA
[3]Center for Quantum Information, IIIS, Tsinghua University, Beijing 100084, People's Republic of China
[4]Condensed Matter Theory Center, Department of Physics, University of Maryland, College Park, Maryland 20742, USA
[5]Department of Physics, Colorado School of Mines, Golden, Colorado 80401, USA

(Received 28 September 2018; published 20 December 2018)

We study the nonequilibrium dynamics of Abelian anyons in a one-dimensional system. We find that the interplay of anyonic statistics and interactions gives rise to spatially asymmetric particle transport together with a novel dynamical symmetry that depends on the anyonic statistical angle and the sign of interactions. Moreover, we show that anyonic statistics induces asymmetric spreading of quantum information, characterized by asymmetric light cones of out-of-time-ordered correlators. Such asymmetric dynamics is in sharp contrast to the dynamics of conventional fermions or bosons, where both the transport and information dynamics are spatially symmetric. We further discuss experiments with cold atoms where the predicted phenomena can be observed using state-of-the-art technologies. Our results pave the way toward experimentally probing anyonic statistics through nonequilibrium dynamics.

DOI: 10.1103/PhysRevLett.121.250404

Fundamental particles in nature can be classified as either bosons or fermions, depending on their exchange statistics. However, other types of quantum statistics are possible in certain circumstances. For instance, Abelian anyons are characterized by fractional statistics interpolating between bosons and fermions [1–5]. When two anyons are exchanged, their joint wave function picks up a generic phase factor, $e^{i\theta}$. Anyons play important roles in several areas of modern physics research, such as fractional quantum Hall systems [5–7] and spin liquids [8–10], not only because of their fundamental physical interest, but also due to their potential applications in topological quantum computation and information processing [11–17]. In the beginning, the exploration of anyons was restricted to two-dimensional systems. Later, Haldane generalized the concept of fractional statistics and anyons to arbitrary dimensions [18,19].

The physics of Abelian anyons in one dimension (1D) has attracted a great deal of recent interest [20–36]. Anyons in 1D exhibit a number of intriguing properties, including statistics-induced quantum phase transitions [37–40], asymmetric momentum distribution in ground states [32–37,41], continuous fermionization of bosonic atoms [42], and anyonic symmetry protected topological phases [41]. Several schemes have been proposed for implementing anyonic statistics in ultracold atoms [37,38,41–43] and photonic systems [44] by engineering occupation-number dependent hopping using Raman-assisted tunneling [37,38] or periodic driving [42,44]. Cold atom quantum systems [45–47] are powerful platforms not only for probing equilibrium properties of many-body systems, but also for studying uncharted nonequilibrium physics [48–57]. Yet, most of the nonequilibrium studies to date have focused on fermionic or bosonic systems, where anyonic statistics do not come into play.

In this work, we study the interplay between anyonic statistics and nonequilibrium dynamics. In particular, we study the particle transport and information dynamics of Abelian anyons in 1D, motivated by recent proposals [37,38,41,42] and the experimental realization of density-dependent tunneling [43,58], as well as by technological advances in probing nonequilibrium dynamics in ultracold atomic systems [50,51]. As we shall see, statistics plays an important role in the nonequilibrium dynamics of anyons. First, distinct from the bosonic and fermionic cases, anyons in 1D exhibit *asymmetric* density expansion under time evolution of a homogeneous anyon-Hubbard model (AHM). The asymmetric transport is controlled by the anyonic statistical angle θ and interaction strength U. When the sign of θ or U is reversed, the expansion changes its preferred direction, thus revealing a novel dynamical symmetry of the underlying AHM. We identify this symmetry operator and analyze the asymmetric expansion dynamics using perturbation theory, confirming the important role played by statistics and interactions. In addition, we use the so-called out-of-time-ordered correlator (OTOC) [59] to characterize the spreading of information in such systems. We find that information spreads with different velocities in the left and right directions, forming an asymmetric light cone.

In contrast to previous studies on ground-state properties [30,33–35,37,38,41,42] or hard-core cases [29,36,60] of

one-dimensional anyons, here we focus on the out-of-equilibrium physics of anyonic systems which can be implemented in experiment [37,38,41–43]. Moreover, we focus mainly on observables that both reveal anyonic properties directly and can be probed in cold atom systems, where the anyonic statistics can be realized via correlated-tunneling terms [42]. Crucially, our work provides a new method for detecting anyonic statistics even in systems where the ground state is difficult to prepare.

Model.—We consider one-dimensional lattice anyons with on-site interactions—the anyon-Hubbard model [37,38,41–44]:

$$\hat{H}_A = -J\sum_{j=1}^{L-1}(\hat{a}_j^\dagger \hat{a}_{j+1} + \text{H.c.}) + \frac{U}{2}\sum_{j=1}^{L}\hat{n}_j(\hat{n}_j - 1), \tag{1}$$

where $\hat{n}_j = \hat{a}_j^\dagger \hat{a}_j$ and J and U describe nearest-neighbor tunneling and on-site interaction, respectively. Throughout the Letter, we set $J = 1$ as the energy unit. The anyon creation ($\hat{a}_j^\dagger$) and annihilation ($\hat{a}_j$) operators obey the generalized commutation relations

$$[\hat{a}_j, \hat{a}_k]_\theta \equiv \hat{a}_j\hat{a}_k - e^{-i\theta\,\mathrm{sgn}(j-k)}\hat{a}_k\hat{a}_j = 0, \tag{2}$$

$$[\hat{a}_j, \hat{a}_k^\dagger]_{-\theta} \equiv \hat{a}_j\hat{a}_k^\dagger - e^{i\theta\,\mathrm{sgn}(j-k)}\hat{a}_k^\dagger\hat{a}_j = \delta_{jk}, \tag{3}$$

where θ is the anyonic statistical angle. Here, $\mathrm{sgn}(k) = -1$, 0, 1 for $k < 0, = 0, > 0$, respectively. Equations (2) and (3) imply that particles on the same site behave as bosons. When $\theta = \pi$, these lattice anyons are "pseudofermions," as they behave like fermions off site, while being bosons on site [37].

By a generalized, fractional Jordan-Wigner transformation, $\hat{a}_j = \hat{b}_j e^{-i\theta\sum_{k=1}^{j-1}\hat{n}_k}$, the above AHM can be mapped to an extended Bose-Hubbard model (EBHM),

$$\hat{H}_B = -J\sum_{j=1}^{L-1}(\hat{b}_j^\dagger \hat{b}_{j+1}e^{-i\theta\hat{n}_j} + \text{H.c.}) + \frac{U}{2}\sum_{j=1}^{L}\hat{n}_j(\hat{n}_j - 1), \tag{4}$$

where $\hat{b}_j$ is the bosonic annihilation operator for site j, and $\hat{n}_j = \hat{a}_j^\dagger\hat{a}_j = \hat{b}_j^\dagger\hat{b}_j$ [26–28,37,38,42]. Under this transformation, anyonic statistics have been translated to density-dependent hopping terms, which are the key ingredient to implementing anyonic statistics in 1D. As mentioned, one can realize such terms in cold atomic systems using either Raman-assisted tunneling [37,38] or time-periodic driving [42–44].

Asymmetric particle transport.—We consider the expansion dynamics of anyons initially localized at the central region of a 1D lattice, one per occupied site. The initial state can be written as a product state in Fock space, $|\Psi_0\rangle_A = \prod_i \hat{a}_i^\dagger|0\rangle$, with occupied sites distributed symmetrically around the lattice center. At times $t > 0$, the system evolves under $\hat{H}_A$ [Eq. (1)]. This procedure is equivalent to a quantum quench from $U/J = \infty$ to finite U/J. To characterize particle transport, we study the dynamics of the *real* space anyon density, $n_j^A(t) = {}_A\langle\Psi_0|e^{i\hat{H}_A t}\hat{n}_j e^{-i\hat{H}_A t}|\Psi_0\rangle_A$, where we have set $\hbar = 1$. Under the fractional Jordan-Wigner transformation, the particle number operator $\hat{n}_j$ remains invariant (i.e., $\hat{a}_j^\dagger\hat{a}_j = \hat{b}_j^\dagger\hat{b}_j$), $\hat{H}_A$ maps to $\hat{H}_B$, and the initial state picks up an unimportant phase ϕ, i.e., $|\Psi_0\rangle_A = e^{i\phi}\prod_i \hat{b}_i^\dagger|0\rangle = e^{i\phi}|\Psi_0\rangle_B$. These relations directly lead to the following equality:

$$n_j^A(t) = {}_B\langle\Psi_0|e^{i\hat{H}_B t}\hat{n}_j e^{-i\hat{H}_B t}|\Psi_0\rangle_B = n_j^B(t), \tag{5}$$

which indicates that anyonic and bosonic particle densities are equivalent under time evolution governed by their respective initial states and Hamiltonians. Equation (5) maps anyonic density to bosonic density, which can be directly measured in cold atom experiments [37,38,41,42,50,51].

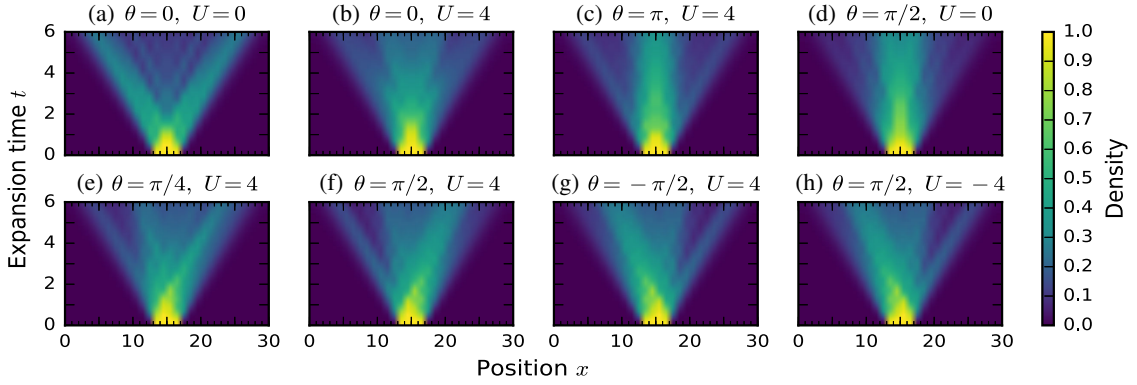

FIG. 1. Density expansion dynamics for particles initially localized one per site in the central N sites, with different statistical angles θ and interaction strengths U. In all plots, the particle number is $N = 4$ and the lattice size is $L = 30$. (a)–(b) Bosonic cases with zero and nonzero interactions, respectively. (c) Pseudofermionic case ($\theta = \pi$) with nonzero interactions. (d)–(h) Anyonic cases with various values for θ and U.

Likewise, the state $|\Psi_0\rangle_B$ can be easily prepared in such experiments [50,51].

Exact diagonalization results on the expansion dynamics for a variety of statistical angles and interaction strengths are shown in Fig. 1. Figures 1(a) and 1(b) show transport dynamics for the bosonic case ($\theta = 0$). Consistent with experimental observations in Ref. [51], bosons exhibit ballistic expansion when $U = 0$ [Fig. 1(a)]. However, any finite interaction strength ($U \neq 0$) breaks the integrability of the Bose-Hubbard model and dramatically suppresses the density expansion [Fig. 1(b)], leading to diffusive (i.e., nonballistic) dynamics [51]. In contrast to bosonic cases, for anyons with nonzero θ and even *vanishing* interaction strength, the transport shows strong signatures of being diffusive rather than ballistic [see Fig. 1(d)]. This implies that anyonic statistics itself can break integrability and act as a form of effective interaction [61], as is immediately clear from the correlated-tunneling terms in the EBHM in Eq. (4). From Figs. 1(a) and 1(d) we also note that for bosons or anyons with zero interaction strength, the density expansion is symmetric.

Different from the above symmetric transport, for anyons with $0 < \theta < \pi$ and finite interaction strength U, the dynamical density distribution is asymmetric, with one preferred propagation direction [Figs. 1(e)–1(h)]. This is the most striking feature of anyonic statistics' effects on transport behavior. Such asymmetric expansion is due to inversion symmetry breaking of the AHM [37,62], a direct consequence of the underlying 1D anyonic statistics [Eqs. (2) and (3)]. A perturbation analysis reveals the important role played by statistics and interactions (see Supplemental Material for details [63]). Our results illustrate that anyonic statistics has clear signatures in nonequilibrium transport, which may aid in their detection. Previous works have suggested detecting anyonic statistics via asymmetric momentum distributions in equilibrium ground states [33–38,42], but ground states are often difficult to prepare experimentally.

Figure 2(a) plots one measure of the above-mentioned asymmetry, the particle number difference $\Delta N = \sum_{i=1}^{L/2}(n_{i+L/2} - n_i)$ between two halves versus statistical angle θ. The results indeed show clear dependence on the statistical parameter θ, thus demonstrating that one can detect the underlying anyonic statistics using expansion dynamics. Figure 2(b) shows the dependence of ΔN on interaction strength for a fixed statistical angle. We note that the largest asymmetric measure ΔN occurs for intermediate values of U, as the expansion dynamics are symmetric at both $U = 0$ (analyzed below) as well as in the limit of large U (the hard-core case) [29,36,60].

Symmetry analysis.—Comparing Figs. 1(g) and 1(h) to Fig. 1(f), we can clearly see that by reversing the sign of the statistical angle θ or interaction strength U, anyons also reverse their preferred propagation direction. This dynamical symmetry is further illustrated in Figs. 2(a) and 2(b),

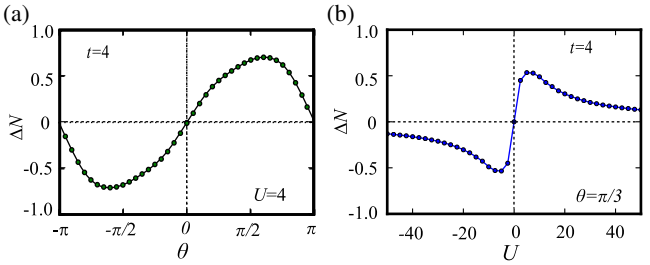

FIG. 2. (a) Particle number difference ΔN between the right and left halves versus anyon angle θ at time $t = 4$, which is beyond the perturbative regime yet occurs before the quench hits the boundary. The interaction strength is $U = 4$. (b) ΔN versus interaction strength U at time $t = 4$, with $\theta = \pi/3$. The particle number is $N = 4$, and the lattice size is $L = 30$ for both plots, just as in Fig. 1.

which provide evidence that ΔN is indeed an odd function of θ and an odd function of U. The results differ from experimental findings for fermionic or bosonic gases [50,51], where density expansion dynamics are identical for $\pm U$ (further analyzed in a recent theoretical work, Ref. [64]).

To understand the dynamical symmetry, we focus on the symmetry properties of the mapped EBHM for convenience. $\hat{H}_B$ explicitly breaks inversion symmetry $\mathcal{I}$, as the phase of the correlated-tunneling term depends only on the occupation number of the left site (which becomes the right site under inversion). It also breaks time-reversal symmetry, as $\mathcal{T} e^{-i\theta\hat{n}_j}\mathcal{T}^{-1} = e^{i\theta\hat{n}_j}$. However, if we consider the number-dependent gauge transformation $\mathcal{R} = e^{-i\theta\sum_j \hat{n}_j(\hat{n}_j-1)/2}$ and define a new symmetry operator $\mathcal{K} = \mathcal{R}\mathcal{I}\mathcal{T}$, $\hat{H}_B$ is invariant under $\mathcal{K}$ [41,63]:

$$\mathcal{K}\hat{H}_B\mathcal{K}^\dagger = \hat{H}_B. \tag{6}$$

The transformed EBHMs with the opposite sign of interaction or statistical angle are related by the number parity operator $\mathcal{P} = e^{i\pi\sum_r \hat{n}_{2r+1}}$ or the time-reversal operator $\mathcal{T}$, respectively,

$$\mathcal{P}\hat{H}_{B,+U}\mathcal{P}^\dagger = -\hat{H}_{B,-U}, \tag{7}$$

$$\mathcal{T}\hat{H}_{B,+\theta}\mathcal{T}^{-1} = \hat{H}_{B,-\theta}. \tag{8}$$

Using Eqs. (6)–(8), one can derive the following relations [63]:

$$\langle\hat{n}_j(t)\rangle_{+U} = \langle\hat{n}_{j'}(t)\rangle_{-U}, \tag{9}$$

$$\langle\hat{n}_j(t)\rangle_{+\theta} = \langle\hat{n}_{j'}(t)\rangle_{-\theta}, \tag{10}$$

where $\langle\cdot\rangle$ denotes the expectation value of a Heisenberg operator taken with respect to the initial state given above,

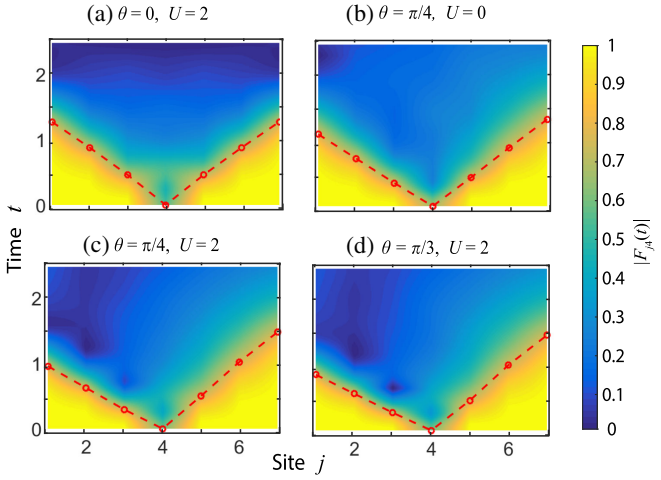

FIG. 3. OTOC growth $|F_{jk}(t)|$ for different statistical angles θ and interaction strengths U. Here, $L = 7$, $\beta^{-1} = 6$, $k = 4$, and the local Hilbert space of each site is truncated to three states. Plotted is (a) a bosonic case ($\theta = 0$) with nonzero interaction, as well as anyonic cases with (b) vanishing and (c), (d) nonvanishing interaction strengths. The red dots denote where the OTOCs fall to 75% of their initial values. The color maps are interpolated to noninteger j to better illustrate the light cone behavior.

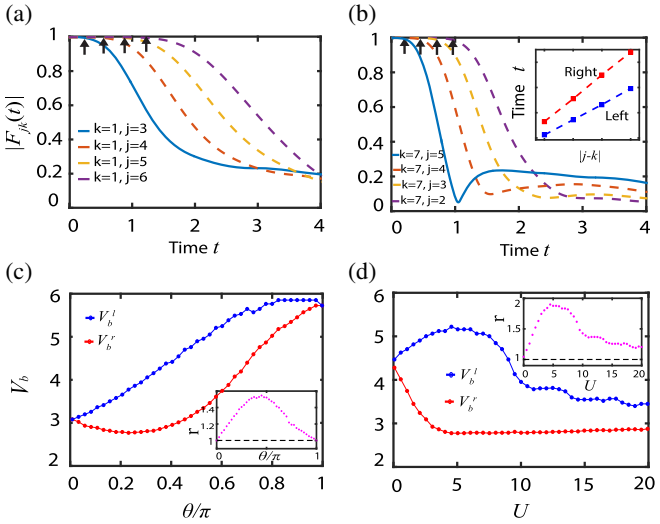

FIG. 4. (a) OTOC growth characterizing quantum information spreading from the leftmost site, $k = 1$, rightward. The OTOC starts to fall when information reaches the jth site, and the black arrows denote the OTOCs' fall to 99% of their initial values. Parameters: $\theta = \pi/3$, $U = 2$, $L = 7$. (b) Same as (a) but shows information spreading from the rightmost site $k = 7$ toward the left. Inset: linear fit to extract the butterfly velocities for left (blue) and right (red) directions, respectively. (c) Left (V_b^l) and right (V_b^r) butterfly velocities' dependence on statistical angle θ when $U = 2$. Inset: velocity ratio $r = V_b^l/V_b^r$ versus angle θ. (d) Dependence of V_b^l and V_b^r on interaction strength U when $\theta = \pi/2$. Inset: velocity ratio $r = V_b^l/V_b^r$ versus interaction strength U.

and sites j, j' are related by the inversion operator $\mathcal{I}$. In fact, the above equations hold for a more general class of initial states (see Supplemental Material [63]). Therefore, in contrast to fermionic or bosonic gases [64] (symmetric expansion), the above relations indicate that anyons flip their preferred expansion direction when one changes the sign of U or θ in Eq. (1). The above equalities also immediately imply when $\theta = 0$ or π (bosons or pseudofermions, respectively) or when $U = 0$, the transport is symmetric [shown in Figs. 1(a)–1(d)], consistent with previous results for integrable systems [29,36,60].

Information dynamics.—The spreading of information in an interacting quantum many-body system has received tremendous interest [48,65–70]. For conventional fermionic or bosonic systems with translation invariance, information spreading occurs in a spatially symmetric way [66–68]. However, as we demonstrate below, this is not generally the case for anyonic systems, where statistics can manifest itself in the information dynamics.

We diagnose information spreading by examining the OTOC, a quantity that has received a great deal of recent interest in studies of quantum scrambling [69–81]. We define the anyonic OTOC as $C_{jk}(t) = \langle |[\hat{a}_j(t), \hat{a}_k(0)]_\theta|^2 \rangle_\beta$. Here, $\langle\cdot\rangle_\beta$ is taken with respect to the thermal ensemble $e^{-\beta \hat{H}_A}/\mathrm{tr}(e^{-\beta \hat{H}_A})$ with inverse temperature β. The use of the generalized commutator defined by Eqs. (2) and (3) ensures that $C_{jk}(t)$ vanishes at $t = 0$. It then starts to grow when quantum information propagates from site k to site j [68–71]. We focus on the out-of-time-ordered part of the above commutator,

$$F_{jk}(t) = \langle \hat{a}_j^\dagger(t)\hat{a}_k^\dagger(0)\hat{a}_j(t)\hat{a}_k(0)\rangle_\beta e^{i\theta \mathrm{sgn}(j-k)}. \quad (11)$$

Figures 3(a)–3(d) show numerical results for various interaction strengths U and statistical angles θ. In contrast to the density transport shown in Fig. 1(b), quantum information spreads in a ballistic way for bosons even when $U \neq 0$ [66,67]. Indeed, for bosons ($\theta = 0$), the OTOCs map out a symmetric light cone, as shown in Fig. 3(a). However, for the anyonic case ($\theta \neq 0$, π), information propagation is asymmetric for the left and right directions [Figs. 3(b)–3(d)], resulting in an asymmetric light cone. We emphasize that this occurs even when $U = 0$, as the aforementioned dynamical symmetry [Eqs. (9) and (10)] does not hold for the OTOC.

Figures 4(a) and 4(b) further illustrate the OTOC's growth for right and left propagation directions, respectively, with $\theta = \pi/3$ and $U = 2$. Indeed, information clearly propagates faster from right to left [Fig. 4(b)] than from left to right [Fig. 4(a)]. In order to extract the butterfly velocities most accurately in a finite-size system, we choose the leftmost site as the reference point for probing information spreading rightward (and vice versa for information spreading leftward). We define a butterfly velocity V_b by the boundary of the space-time region where $|F_{jk}(t)|$

is suppressed by at least 1% of its initial value. The linear fits of butterfly velocities $V_b^{l,r}$ for two directions are shown in the inset of Fig. 4(b). The extracted velocities' dependence on θ and U are further illustrated in Figs. 4(c) and 4(d), respectively. As the results show, when $U > 0$ and $0 < \theta < \pi$, the left information propagation velocity is always larger than the right one, with the greatest disparity at intermediate values of U and θ.

Experimental detection.—To study the transport and information dynamics of the AHM, one can experimentally realize the transformed EBHM. As mentioned, the correlated-tunneling terms in $\hat{H}_B$ can be engineered using laser-assisted tunneling [37,38] or lattice shaking [42–44]. Particle transport can be studied using similar protocols as in previous experiments [50,51], where bosonic atoms are first loaded in the center of a one-dimensional optical lattice before being allowed to move under a homogeneous bosonic Hamiltonian. The time-dependent densities, as measured by absorption imaging, directly reflect the anyons' expansion dynamics. On the other hand, measurement of the OTOC defined by Eq. (11) is more challenging than mapping out the atomic density. However, instead of measuring Eq. (11), one can focus on a bosonic OTOC, $\tilde{F}_{jk}(t) = \langle \hat{b}_j^\dagger(t)\hat{b}_k^\dagger(0)\hat{b}_j(t)\hat{b}_k(0)\rangle$, which, by recent proposals, is experimentally accessible by inverting the sign of $\hat{H}_B$ [82–84] or by preparing two identical copies of the system [68,69]. Numerics show that $\tilde{F}_{jk}(t)$ can also capture the asymmetric features of OTOC growth [63], thus reflecting anyonic statistics' effect on information dynamics, albeit in an indirect way.

Conclusion and outlook.—We have studied nonequilibrium dynamics of Abelian anyons in a 1D system and found that statistics plays a crucial role in both particle transport and information dynamics. Our work provides a novel method for detecting anyonic statistics using nonequilibrium dynamics in ultracold atom systems [43].

We note the intriguing possibility that a similar dynamical symmetry may exist in other models, such as the $\mathbb{Z}_n$ chiral clock model [85,86], which has symmetry properties similar to the AHM. Finally, we point out that the inversion symmetry breaking associated with anyonic statistics is also present for non-Abelian anyons in quasi-1D systems [87–89]—for example, Majorana fermions (or, more generally, parafermions) at the edge of (fractional) quantum Hall systems, in deep connection with the underlying chirality. We hope this study could motivate future investigation of out-of-equilibrium dynamics and chiral information propagation in these topological systems.

We thank Chris Flower and Tobias Grass for helpful discussions. This work was supported by AFOSR, ARO, NSF PFC at JQI, ARO MURI, ARL CDQI, NSF QIS, NSF Ideas Lab on Quantum Computing, the DOE ASCR Quantum Testbed Pathfinder program, and the DOE BES Materials and Chemical Sciences Research for Quantum Information Science program. J. R. G. was supported by the NIST NRC Research Postdoctoral Associateship Award. D. L. D. acknowledges support from the Laboratory for Physical Sciences, Microsoft, and the start-up fund from Tsinghua University. Z. X. G. acknowledges the start-up fund support from Colorado School of Mines. This work was performed in part at the Aspen Center for Physics, which is supported by National Science Foundation Grant No. PHY-1607611. The authors acknowledge the University of Maryland supercomputing resources made available for conducting the research reported in this Letter.

[1] J. M. Leinaas and J Myrheim, On the theory of identical particles, Nuovo Cimento Soc. Ital. Fis. B **37**, 1 (1977).
[2] G. A. Goldin, R. Menikoff, and D. H. Sharp, Representations of a local current algebra in nonsimply connected space and the Aharonov–Bohm effect, J. Math. Phys. **22**, 1664 (1981).
[3] F. Wilczek, Magnetic Flux, Angular Momentum, and Statistics, Phys. Rev. Lett. **48**, 1144 (1982).
[4] D. C. Tsui, H. L. Stormer, and A. C. Gossard, Two-Dimensional Magnetotransport in the Extreme Quantum Limit, Phys. Rev. Lett. **48**, 1559 (1982).
[5] R. B. Laughlin, Anomalous Quantum Hall Effect: An Incompressible Quantum Fluid with Fractionally Charged Excitations, Phys. Rev. Lett. **50**, 1395 (1983).
[6] B. I. Halperin, Statistics of Quasiparticles and the Hierarchy of Fractional Quantized Hall States, Phys. Rev. Lett. **52**, 1583 (1984).
[7] D. Arovas, J. R. Schrieffer, and F. Wilczek, Fractional Statistics and the Quantum Hall Effect, Phys. Rev. Lett. **53**, 722 (1984).
[8] A. Kitaev, Anyons in an exactly solved model and beyond, Ann. Phys. (Amsterdam) **321**, 2 (2006).
[9] H. Yao and S. A. Kivelson, Exact Chiral Spin Liquid with Non-Abelian Anyons, Phys. Rev. Lett. **99**, 247203 (2007).
[10] B. Bauer, L. Cincio, B. P. Keller, M. Dolfi, G. Vidal, S. Trebst, and A. W. W. Ludwig, Chiral spin liquid and emergent anyons in a Kagome lattice Mott insulator, Nat. Commun. **5**, 5137 (2014).
[11] A. Y. Kitaev, Fault-tolerant quantum computation by anyons, Ann. Phys. (Amsterdam) **303**, 2 (2003).
[12] S. D. Sarma, M. Freedman, and C. Nayak, Topologically Protected Qubits from a Possible Non-Abelian Fractional Quantum Hall State, Phys. Rev. Lett. **94**, 166802 (2005).
[13] P. Bonderson, A. Kitaev, and K. Shtengel, Detecting Non-Abelian Statistics in the $\nu = 5/2$ Fractional Quantum Hall State, Phys. Rev. Lett. **96**, 016803 (2006).
[14] A. Stern and B. I. Halperin, Proposed Experiments to Probe the Non-Abelian $\nu = 5/2$ Quantum Hall State, Phys. Rev. Lett. **96**, 016802 (2006).
[15] C. Nayak, S. H. Simon, A. Stern, M. Freedman, and S. D. Sarma, Non-Abelian anyons and topological quantum computation, Rev. Mod. Phys. **80**, 1083 (2008).
[16] J. Alicea, Y. Oreg, G. Refael, F. von Oppen, and M. P. A. Fisher, Non-Abelian statistics and topological quantum

information processing in 1D wire networks, Nat. Phys. **7**, 412 (2011).
[17] A. Stern and N. H. Lindner, Topological quantum computation—From basic concepts to first experiments, Science **339**, 1179 (2013).
[18] F. D. M. Haldane, Fractional Statistics in Arbitrary Dimensions: A Generalization of the Pauli Principle, Phys. Rev. Lett. **67**, 937 (1991).
[19] F. D. M. Haldane, Spinon Gas Description of the $S = 1/2$ Heisenberg Chain with Inverse-Square Exchange: Exact Spectrum and Thermodynamics, Phys. Rev. Lett. **66**, 1529 (1991).
[20] Z. N. C. Ha, Exact Dynamical Correlation Functions of Calogero-Sutherland Model and One-Dimensional Fractional Statistics, Phys. Rev. Lett. **73**, 1574 (1994).
[21] M. V. N. Murthy and R. Shankar, Thermodynamics of a One-Dimensional Ideal Gas with Fractional Exclusion Statistics, Phys. Rev. Lett. **73**, 3331 (1994).
[22] Y.-S. Wu and Y. Yu, Bosonization of One-Dimensional Exclusons and Characterization of Luttinger Liquids, Phys. Rev. Lett. **75**, 890 (1995).
[23] L. Amico, A. Osterloh, and U. Eckern, One-dimensional XXZ model for particles obeying fractional statistics, Phys. Rev. B **58**, R1703 (1998).
[24] L. Mazza, J. Viti, M. Carrega, D. Rossini, and A. De Luca, Energy transport in an integrable parafermionic chain via generalized hydrodynamics, Phys. Rev. B **98**, 075421 (2018).
[25] N. T. Zinner, Strongly interacting mesoscopic systems of anyons in one dimension, Phys. Rev. A **92**, 063634 (2015).
[26] A. Kundu, Exact Solution of Double δ Function Bose Gas Through an Interacting Anyon Gas, Phys. Rev. Lett. **83**, 1275 (1999).
[27] M. T. Batchelor, X.-W. Guan, and N. Oelkers, One-Dimensional Interacting Anyon Gas: Low-Energy Properties and Haldane Exclusion Statistics, Phys. Rev. Lett. **96**, 210402 (2006).
[28] M. D. Girardeau, Anyon-Fermion Mapping and Applications to Ultracold Gases in Tight Waveguides, Phys. Rev. Lett. **97**, 100402 (2006).
[29] A. del Campo, Fermionization and bosonization of expanding one-dimensional anyonic fluids, Phys. Rev. A **78**, 045602 (2008).
[30] P. Calabrese and M. Mintchev, Correlation functions of one-dimensional anyonic fluids, Phys. Rev. B **75**, 233104 (2007).
[31] V. Zatloukal, L. Lehman, S. Singh, J. K. Pachos, and G. K. Brennen, Transport properties of anyons in random topological environments, Phys. Rev. B **90**, 134201 (2014).
[32] M. Greiter, Statistical phases and momentum spacings for one-dimensional anyons, Phys. Rev. B **79**, 064409 (2009).
[33] Y. Hao, Y. Zhang, and S. Chen, Ground-state properties of one-dimensional anyon gases, Phys. Rev. A **78**, 023631 (2008).
[34] Y. Hao, Y. Zhang, and S. Chen, Ground-state properties of hard-core anyons in one-dimensional optical lattices, Phys. Rev. A **79**, 043633 (2009).
[35] G. Tang, S. Eggert, and A. Pelster, Ground-state properties of anyons in a one-dimensional lattice, New J. Phys. **17**, 123016 (2015).
[36] Y. Hao and S. Chen, Dynamical properties of hard-core anyons in one-dimensional optical lattices, Phys. Rev. A **86**, 043631 (2012).
[37] T. Keilmann, S. Lanzmich, I. McCulloch, and M. Roncaglia, Statistically induced phase transitions and anyons in 1D optical lattices, Nat. Commun. **2**, 361 (2011).
[38] S. Greschner and L. Santos, Anyon Hubbard Model in One-Dimensional Optical Lattices, Phys. Rev. Lett. **115**, 053002 (2015).
[39] J. Arcila-Forero, R. Franco, and J. Silva-Valencia, Critical points of the anyon-Hubbard model, Phys. Rev. A **94**, 013611 (2016).
[40] J. Arcila-Forero, R. Franco, and J. Silva-Valencia, Three-body-interaction effects on the ground state of one-dimensional anyons, Phys. Rev. A **97**, 023631 (2018).
[41] F. Lange, S. Ejima, and H. Fehske, Anyonic Haldane Insulator in One Dimension, Phys. Rev. Lett. **118**, 120401 (2017).
[42] C. Sträter, S. C. L. Srivastava, and A. Eckardt, Floquet Realization and Signatures of One-Dimensional Anyons in an Optical Lattice, Phys. Rev. Lett. **117**, 205303 (2016).
[43] L. W. Clark, B. M. Anderson, L. Feng, A. Gaj, K. Levin, and C. Chin, Observation of Density-Dependent Gauge Fields in a Bose-Einstein Condensate Based on Micromotion Control in a Shaken Two-Dimensional Lattice, Phys. Rev. Lett. **121**, 030402 (2018).
[44] L. Yuan, M. Xiao, S. Xu, and S. Fan, Creating anyons from photons using a nonlinear resonator lattice subject to dynamic modulation, Phys. Rev. A **96**, 043864 (2017).
[45] M. Greiner, O. Mandel, T. Esslinger, T. W. Hänsch, and I. Bloch, Quantum phase transition from a superfluid to a Mott insulator in a gas of ultracold atoms, Nature (London) **415**, 39 (2002).
[46] M. Lewenstein, A. Sanpera, V. Ahufinger, B. Damski, A. Sen, and U. Sen, Ultracold atomic gases in optical lattices: Mimicking condensed matter physics and beyond, Adv. Phys. **56**, 243 (2007).
[47] I. Bloch, J. Dalibard, and W. Zwerger, Many-body physics with ultracold gases, Rev. Mod. Phys. **80**, 885 (2008).
[48] J. Eisert, M. Friesdorf, and C. Gogolin, Quantum many-body systems out of equilibrium, Nat. Phys. **11**, 124 (2015).
[49] C. Gogolin and J. Eisert, Equilibration, thermalisation, and the emergence of statistical mechanics in closed quantum systems, Rep. Prog. Phys. **79**, 056001 (2016).
[50] U. Schneider, L. Hackermüller, J. P. Ronzheimer, S. Will, S. Braun, T. Best, I. Bloch, E. Demler, S. Mandt, D. Rasch, and A. Rosch, Fermionic transport and out-of-equilibrium dynamics in a homogeneous Hubbard model with ultracold atoms, Nat. Phys. **8**, 213 (2012).
[51] J. P. Ronzheimer, M. Schreiber, S. Braun, S. S. Hodgman, S. Langer, I. P. McCulloch, F. Heidrich-Meisner, I. Bloch, and U. Schneider, Expansion Dynamics of Interacting Bosons in Homogeneous Lattices in One and Two Dimensions, Phys. Rev. Lett. **110**, 205301 (2013).
[52] D. Pertot, A. Sheikhan, E. Cocchi, L. A. Miller, J. E. Bohn, M. Koschorreck, M. Köhl, and C. Kollath, Relaxation Dynamics of a Fermi Gas in an Optical Superlattice, Phys. Rev. Lett. **113**, 170403 (2014).

[53] C.-L. Hung, V. Gurarie, and C. Chin, From cosmology to cold atoms: Observation of Sakharov oscillations in a quenched atomic superfluid, Science **341**, 1213 (2013).

[54] A. M. Kaufman, M. E. Tai, A. Lukin, M. Rispoli, R. Schittko, P. M. Preiss, and M. Greiner, Quantum thermalization through entanglement in an isolated many-body system, Science **353**, 794 (2016).

[55] J. Zhang, G. Pagano, P. W. Hess, A. Kyprianidis, P. Becker, H. Kaplan, A. V. Gorshkov, Z.-X. Gong, and C. Monroe, Observation of a many-body dynamical phase transition with a 53-qubit quantum simulator, Nature (London) **551**, 601 (2017).

[56] N. Fläschner, D. Vogel, M. Tarnowski, B. S. Rem, D.-S. Lühmann, M. Heyl, J. C. Budich, L. Mathey, K. Sengstock, and C. Weitenberg, Observation of dynamical vortices after quenches in a system with topology, Nat. Phys. **14**, 265 (2018).

[57] P. Jurcevic, H. Shen, P. Hauke, C. Maier, T. Brydges, C. Hempel, B. P. Lanyon, M. Heyl, R. Blatt, and C. F. Roos, Direct Observation of Dynamical Quantum Phase Transitions in an Interacting Many-Body System, Phys. Rev. Lett. **119**, 080501 (2017).

[58] F. Meinert, M. J. Mark, K. Lauber, A. J. Daley, and H.-C. Nägerl, Floquet Engineering of Correlated Tunneling in the Bose-Hubbard Model with Ultracold Atoms, Phys. Rev. Lett. **116**, 205301 (2016).

[59] A. I. Larkin and Y. N. Ovchinnikov, Quasiclassical method in the theory of superconductivity, J. Exp. Theor. Phys. **28**, 1200 (1969).

[60] T. M. Wright, M. Rigol, M. J. Davis, and K. V. Kheruntsyan, Nonequilibrium Dynamics of One-Dimensional Hard-Core Anyons Following a Quench: Complete Relaxation of One-Body Observables, Phys. Rev. Lett. **113**, 050601 (2014).

[61] S. C. Morampudi, A. M. Turner, F. Pollmann, and F. Wilczek, Statistics of Fractionalized Excitations Through Threshold Spectroscopy, Phys. Rev. Lett. **118**, 227201 (2017).

[62] F. Wilczek, *Fractional Statistics and Anyon Superconductivity* (World Scientific, Singapore, 1990), Vol. 5.

[63] See Supplemental Material at http://link.aps.org/supplemental/10.1103/PhysRevLett.121.250404 for details on the dynamical symmetry, perturbation calculations, and a comparison between bosonic and anyonic out-of-time-ordered correlators.

[64] J. Yu, N. Sun, and H. Zhai, Symmetry Protected Dynamical Symmetry in the Generalized Hubbard Models, Phys. Rev. Lett. **119**, 225302 (2017).

[65] E. H. Lieb and D. W. Robinson, The finite group velocity of quantum spin systems, Commun. Math. Phys. **28**, 251 (1972).

[66] A. M. Läuchli and C. Kollath, Spreading of correlations and entanglement after a quench in the one-dimensional Bose Hubbard model, J. Stat. Mech. (2008) P05018.

[67] M. Cheneau, P. Barmettler, D. Poletti, M. Endres, P. Schauß, T. Fukuhara, C. Gross, I. Bloch, C. Kollath, and S. Kuhr, Light-cone-like spreading of correlations in a quantum many-body system, Nature (London) **481**, 484 (2012).

[68] A. Bohrdt, C. B. Mendl, M. Endres, and M. Knap, Scrambling and thermalization in a diffusive quantum many-body system, New J. Phys. **19**, 063001 (2017).

[69] H. Shen, P. Zhang, R. Fan, and H. Zhai, Out-of-time-order correlation at a quantum phase transition, Phys. Rev. B **96**, 054503 (2017).

[70] D. J. Luitz and Y. B. Lev, Information propagation in isolated quantum systems, Phys. Rev. B **96**, 020406 (2017).

[71] Y. Huang, Y.-L. Zhang, and X. Chen, Out-of-time-ordered correlators in many-body localized systems, Ann. Phys. (Amsterdam) **529**, 1600318 (2017).

[72] C. W. von Keyserlingk, T. Rakovszky, F. Pollmann, and S. L. Sondhi, Operator Hydrodynamics, OTOCs, and Entanglement Growth in Systems Without Conservation Laws, Phys. Rev. X **8**, 021013 (2018).

[73] A. Nahum, S. Vijay, and J. Haah, Operator Spreading in Random Unitary Circuits, Phys. Rev. X **8**, 021014 (2018).

[74] R.-Q. He and Z.-Y. Lu, Characterizing many-body localization by out-of-time-ordered correlation, Phys. Rev. B **95**, 054201 (2017).

[75] R. Fan, P. Zhang, H. Shen, and H. Zhai, Out-of-time-order correlation for many-body localization, Sci. Bull. **62**, 707 (2017).

[76] Y. Chen, Universal logarithmic scrambling in many body localization, arXiv:1608.02765.

[77] B. Swingle and D. Chowdhury, Slow scrambling in disordered quantum systems, Phys. Rev. B **95**, 060201 (2017).

[78] E. Leviatan, F. Pollmann, J. H. Bardarson, D. A. Huse, and E. Altman, Quantum thermalization dynamics with Matrix-Product States, arXiv:1702.08894.

[79] S. Xu and B. Swingle, Accessing scrambling using matrix product operators, arXiv:1802.00801.

[80] Y.-L. Zhang, Y. Huang, and X. Chen, Information scrambling in chaotic systems with dissipation, arXiv:1802.04492.

[81] B. Swingle and N. Y. Halpern, Resilience of scrambling measurements, Phys. Rev. A **97**, 062113 (2018).

[82] N. Y. Yao, F. Grusdt, B. Swingle, M. D. Lukin, D. M. Stamper-Kurn, J. E. Moore, and E. A. Demler, Interferometric approach to probing fast scrambling, arXiv:1607.01801.

[83] G. Zhu, M. Hafezi, and T. Grover, Measurement of many-body chaos using a quantum clock, Phys. Rev. A **94**, 062329 (2016).

[84] B. Swingle, G. Bentsen, M. Schleier-Smith, and P. Hayden, Measuring the scrambling of quantum information, Phys. Rev. A **94**, 040302 (2016).

[85] R. Samajdar, S. Choi, H. Pichler, M. D. Lukin, and S. Sachdev, Numerical study of the chiral $\mathbb{Z}_3$ quantum phase transition in one spatial dimension, Phys. Rev. A **98**, 023614 (2018).

[86] S. Whitsitt, R. Samajdar, and S. Sachdev, Quantum field theory for the chiral clock transition in one spatial dimension, Phys. Rev. B **98**, 205118 (2018).

[87] D. J. Clarke, J. Alicea, and K. Shtengel, Exotic non-Abelian anyons from conventional fractional quantum Hall states, Nat. Commun. **4**, 1348 (2013).

[88] M. Cheng, Superconducting proximity effect on the edge of fractional topological insulators, Phys. Rev. B **86**, 195126 (2012).

[89] R. S. K. Mong, D. J. Clarke, J. Alicea, N. H. Lindner, P. Fendley, C. Nayak, Y. Oreg, A. Stern, E. Berg, K. Shtengel, and M. P. A. Fisher, Universal Topological Quantum Computation from a Superconductor-Abelian Quantum Hall Heterostructure, Phys. Rev. X **4**, 011036 (2014).